Directed Hydroxyl Radical Probing of 16S Ribosomal RNA in 70S Ribosomes from Internal Positions of the RNA†

Lisa F. Newcomb and Harry F. Noller*

Center for Molecular Biology of RNA, Sinsheimer Laboratories, University of California, Santa Cruz, California 95064

Received July 9, 1998; Revised Manuscript Received November 12, 1998

ABSTRACT: Directed hydroxyl radical probing of 16S ribosomal RNA from Fe(II) tethered to specific sites within the RNA was used to determine RNA−RNA proximities in 70S ribosomes. We have transcribed 16S ribosomal RNA in vitro as two separate fragments, covalently attached an Fe(II) probe to a 5′-guanosine-α-phosphorothioate at the junction between the two fragments, and reconstituted 30S subunits with the two separate pieces of RNA and the small subunit proteins. Reconstituted 30S subunits capable of association with 50S subunits were selected by isolation of 70S ribosomes. Hydroxyl radicals, generated in situ from the tethered Fe(II), cleaved sites in the 16S rRNA backbone that were close in three-dimensional space to the Fe(II), and a primer extension was used to identify these sites of cleavage. Two sets of 16S ribosomal RNA fragments, 1−360/361−1542 and 1−448/449−1542, were reconstituted into active 30S subunits. Fe(II) tethered to position 361 results in cleavage of 16S rRNA around nucleotides 34, 160, 497, 512, 520, 537, 552, and 615, as well as around positions 1410, 1422, 1480, and 1490. Fe(II) tethered to position 449 induces cleavage around nucleotide 488 and around positions 42 and 617. Fe(II) tethered to the 5′ end of 16S rRNA induces cleavage of the rRNA around nucleotides 5, 601, 615, and 642. These results provide constraints for the positioning of these regions of 16S rRNA, for which there has previously been only limited structural information, within the 30S subunit.

The *Escherichia coli* 30S ribosomal subunit is comprised of 16S ribosomal RNA, together with 21 ribosomal proteins. Understanding the three-dimensional structure of this 1542-nucleotide RNA within the ribosome is one of the most challenging problems in structural biology. Its secondary structure was determined by comparative sequence analysis using 16S rRNA[1]-like sequences of different organisms (*1*−*3*). However, determining how the more than 60 individual helical elements of 16S rRNA are arranged in three-dimensional space presents a substantially more challenging problem. To this end, biochemical data from a variety of approaches, including protein footprints (*4*, *5*), protein−RNA cross-links (*6*), and RNA−RNA cross-links (*7*−*9*), have provided low-resolution constraints for the locations of the helices relative to each other and to specific ribosomal proteins, whose centers of mass have been positioned by neutron scattering (*10*). Recently, directed hydroxyl radical probing from ribosomal proteins (*11*, *12*, *13*; G. Culver, unpublished), functional ligands (*14*−*16*), and rRNA (Samaha et al., unpublished) has provided a new approach to obtaining constraints for the folding of 16S rRNA. These data have led to the construction of low-resolution models for the folding of 16S rRNA in the 30S subunit by several groups of investigators (*4*, *8*, *17*−*19*). However, the experimental constraints are not distributed uniformly throughout 16S rRNA. For example, much of the 5′ and 3′ minor domains are poorly constrained and so are not represented in some models (*4*, *18*).

Since many of the poorly constrained features of 16S rRNA lack protein footprints, they most likely constitute RNA-rich regions of the 30S subunit. To obtain structural information about these regions of 16S rRNA we sought to probe RNA−RNA proximities directly from Fe(II) tethered to specific sites within the rRNA. We created a discontinuity in 16S rRNA by transcribing two fragments of the rRNA in vitro. Previously it had been shown that active 30S subunits could be reconstituted using in vitro transcripts of 16S rRNA and the total small subunit proteins (TP30) (*20*). Furthermore, in vitro transcripts corresponding to the 5′, central, and 3′ domains of 16S rRNA have been shown to reconstitute with TP30 into discrete particles (*21*−*23*). In these studies, we reconstituted 30S subunits from two in vitro transcribed fragments of rRNA in which Fe(II) was tethered to GMPS at the 5′ terminus of the 3′ fragment via a 1-(*p*-bromoacetamidobenzyl)-EDTA (BABE) linker (*24*). Initiation of hydroxyl radical formation in situ (*14*) then allowed us to probe the RNA neighborhood around the tethered Fe(II).

We first probed 16S rRNA from Fe(II) tethered to its 5′-terminus. In the second construct that we examined, Fe(II) was tethered to nucleotide 361, which is in an internal loop situated within a three-way helical junction in a region of 16S rRNA for which there are few structural constraints. In the third construct, Fe(II) was tethered to position 449 in an internal loop of low sequence conservation for which there is currently little structural information. These experiments

† This work was supported by NIH Grant No. GM-17129 (to H.F.N.), NIH postdoctoral fellowship No. GM-17532 (to L.F.N.), and a grant to the Center for Molecular Biology of RNA from the Lucille P. Markey Charitable Trust.

* To whom correspondence should be addressed.

[1] Abbreviations: rRNA, ribosomal RNA; EDTA, ethylenediaminetetraacetic acid; BABE, 1-(*p*-bromoacetamidobenzyl)-EDTA; GMPS, guanosine-α-phosphorothioate; GMP, guanosine monophosphate; tRNA, transfer RNA; TP30, total proteins from 30S subunits; PCR, polymerase chain reaction.

10.1021/bi981644a CCC: $18.00
Published on Web 12/29/1998

provide a significant addition to the catalog of available constraints for the folding of 16S rRNA. In particular, they provide information about the positions of rRNA elements in the 5′ and 3′ minor domains that were previously only poorly determined.

MATERIALS AND METHODS

Reagents. Buffer A contains 20 mM NH_4^+-Hepes (pH 7.5), 20 mM $MgCl_2$, and 500 mM NH_4Cl; buffer B contains 20 mM NH_4^+-Hepes (pH 7.5), 10 mM $MgCl_2$, and 100 mM NH_4Cl; buffer C contains 20 mM NH_4^+-Hepes (pH 7.5), 20 mM $MgCl_2$, and 100 mM NH_4Cl. Preparation of 16S rRNA and 30S, 50S, and 70S ribosomes was done as described (*25*). TP30 was prepared from 30S subunits isolated by zonal centrifugation as previously described (*26*) and stored in buffer A. Synthesis of 1-(*p*-bromoacetamidobenzyl)-EDTA (BABE) was done as previously described (*24*).

Preparation of Gene Constructs. The gene encoding 16S rRNA was amplified, either in its entirety or in fragments, from pSTL102 (*27*) by PCR. Primers for the 5′ end of the 1−360 and 1−448 constructs contained the restriction site for *Eco*RI and the T7 promoter; primers for all other constructs contained the restriction site for *Sac*I and the T7 promoter. Primers for the 3′ end of all fragments contained the restriction sites for *Bsa*I and *Bam*HI. Nucleotides A1 and A2 were mutated to Gs to improve the efficiency of in vitro transcription with T7 polymerase. Constructs were ligated into *Bam*HI-, *Kpn*I-, *Eco*RI-digested or *Bam*HI- and *Sac*I-digested pUC118 (USB). DNA sequence analysis confirmed the predicted sequences.

Preparation of 16S rRNA Transcripts in Vitro. In vitro transcripts were generated using T7 RNA polymerase (*28*) from *Bsa* I linearized plasmids described above. To introduce a thiophosphate or monophosphate at the 5′ terminus of the rRNA, transcriptions were carried out in the presence of a 5-fold molar excess of either GMPS or GMP over each NTP (5 mM final concentration) (*14*, *29*). Transcriptions were carried out in buffer containing 40 mM Tris-HCl (pH 7.9 at room temperature), 26 mM $MgCl_2$, 3 mM spermidine, 0.01% Triton X-100, and 5 mM DTT for 2 h at 37 °C. Transcription was stopped by addition of EDTA and SDS to final concentrations of 50 μM and 0.5%, respectively. RNA was purified by successive extractions with phenol and chloroform and chromatography on a G50-Sephadex (Pharmacia) column (1 × 20 cm) eluted with buffer A. Samples were precipitated on ice for 0.5 h with 0.3 M NH_4OAc and 2.5 volumes of ethanol. Precipitated RNA was recovered by centrifugation for 20 min at 4 °C at 10 000 rpm in a JA-20 rotor, washed with 70% ethanol, resuspended in H_2O, and frozen in aliquots.

BABE Modification of rRNA. Fe(II)−BABE was prepared by incubating 11 mM final concentration $Fe(NH_4)_2(SO_4)_2 \cdot 6H_2O$ and 15 mM final concentration BABE, brought to pH 3−4 with diisopropylethylamine, for 1 h at room temperature followed by incubation for 10 min with 2.5 mM final concentration EDTA (S. Joseph, unpublished). Full-length 5′-GMPS-16S rRNA, or a 3′ and a corresponding 5′-GMPS-16S rRNA fragment, was suspended in 100 μL of H_2O at a final concentration of 5.5 μM and heated in a 95 °C water bath for 4 min, followed by rapid addition of ice-cold H_2O to a final concentration of 0.85 μM. Samples were incubated on ice for 15 min and precipitated as described above. The rRNA was resuspended in 28 μL of H_2O and incubated with 4 mM final concentration Fe(II)−BABE in 20 mM NH_4^+-Hepes (pH 8.5) and 20 mM $MgCl_2$ at 37 °C for 45−60 min. Derivatized RNA was removed from Fe(II)−BABE by two phenol extractions and one chloroform extraction followed by ethanol precipitation as described above. Control 5′-GMP rRNA that was treated with Fe(II)−BABE and control 5′-GMPS RNA lacking Fe(II)−BABE were isolated by following similar procedures.

In Vitro Reconstitution of 30S Subunits. In vitro reconstitution was performed essentially as described by Ofengand and co-workers (*20*). Briefly, for a 100 μL reaction, 60 pmol of modified rRNA and 1 molar equiv of TP30 were combined in buffer A containing 0.01% Nikkol and heated sequentially for 15 min at each of the temperatures 40, 43, 46, 48, and 50 °C followed by quick cooling to 4 °C. The resulting mixture was used for subunit association.

Subunit Association and Purification of 70S Ribosomes. Subunits from a 100 μL reconstitution reaction were incubated with 6−12 pmol of natural 50S subunits in buffer containing 50 mM NH_4^+-Hepes (pH 7.5), 15 mM $MgCl_2$, 100 mM NH_4Cl, and 0.002% Nikkol at 37 °C for 30 min. Samples were layered onto 11 mL of 10−40% sucrose gradients prepared in buffer B. Gradients were spun in an SW41 rotor at 32 000 rpm for 15.5 h at 4 °C. Peaks sedimenting with 70S ribosomes were isolated, and sucrose was removed by centrifugation at 4 °C in a JA-20 rotor at 2800 rpm in Centricon 100 microconcentrators using 3−4 sequential 2 mL washes with buffer B for probing or with buffer C for tRNA binding.

tRNA Binding Assays. E. coli $tRNA^{Phe}$ was transcribed from the linearized p67CF10 (*30*) with α-[^{32}P] UTP. Isolated 70S ribosomes (2.5 pmol) in 20 μL of buffer C were activated at 42 °C for 20 min. After 15 min on ice, 7.5 pmol of *E. coli* $tRNA^{Phe}$ (specific activity 31 Ci/mmol), in 5 μL of buffer C, and either 5 μL of 0.5 ug/μL poly(U) in buffer C or, for message-independent binding, buffer C alone, was added. tRNA binding was performed by incubating this mixture at 37 °C for 10 min. The mixture was placed on ice, and 1 mL of cold buffer C was added. Three 300 μL aliquots were filtered on nitrocellulose filters (Millipore). To control for binding that may occur to natural 70S ribosomes resulting from contamination of the 50S subunits, the efficiency of tRNA binding to 2.5 pmol of 50S subunits was tested in an identical manner.

Hydroxyl Radical Probing and Primer Extension. In all probing experiments 70S ribosomes containing each of the two control rRNAs described above as well as BABE-modified rRNA were isolated. Ribosomes were probed by initiating hydroxyl radical formation with 0.01% H_2O_2 and 2 mM ascorbic acid followed by incubating for 10 min on ice (*5*). Reactions were quenched by addition of 0.27 volumes of 0.1 M thiourea (20 mM final concentration) and precipitated with 0.3 M NaOAc, 2.5 volumes of ethanol, and 1 μg of glycogen (10 mg/mL). RNA was isolated and analyzed by primer extension as previously described (*31*).

RESULTS

Reconstitution of Functional 30S Subunits from Fragmented 16S rRNA. E. coli 30S subunits were reconstituted

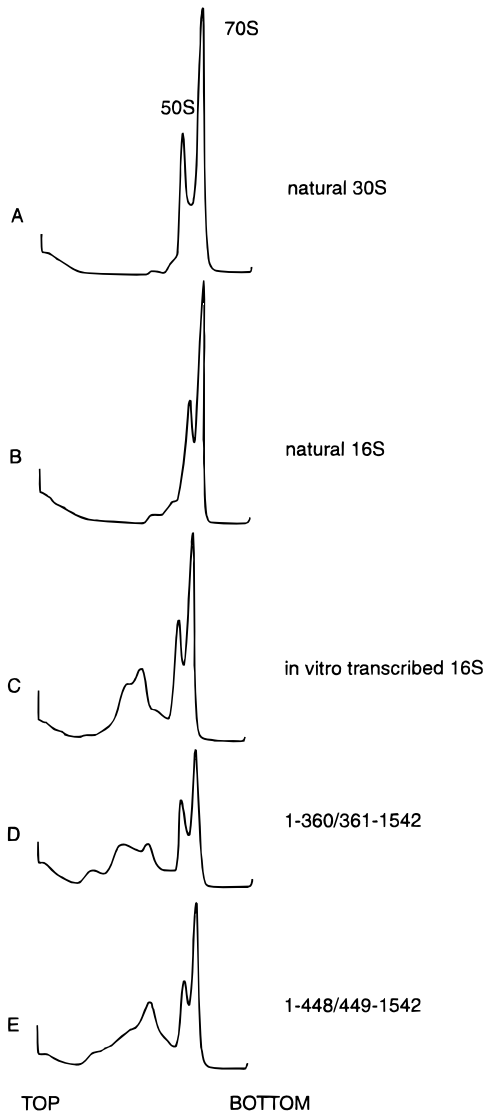

FIGURE 1: Sucrose gradient analysis of 70S ribosomes associated from natural 50S subunits and 30S subunits reconstituted *in vitro* with different constructs of unmodified 16S rRNA: (A) 40 pmol of natural 30S subunits plus 68 pmol 50S subunits; 30S subunits reconstituted with (B) 60 pmol natural 16S rRNA plus 34 pmol 50S subunits, (C) 180 pmol *in vitro* transcribed 16S rRNA plus 31 pmol 50S subunits, (D) 210 pmol 16S rRNA fragments 1−360 and 361−1542 plus 19 pmol 50S subunits, and (E) 210 pmol 16S rRNA fragments 1−448 and 449−1542 plus 19 pmol 50S subunits. Sedimentation is from left to right, and absorbance was monitored at 254 nm.

in vitro from synthetic 16S rRNA, 16S rRNA fragments 1−360 and 361−1542, or the fragments 1−448 and 449−1542, and TP30. To select for functional subunits, reconstituted 30S particles were combined with 50S subunits and the resulting 70S ribosomes were isolated by sucrose gradient sedimentation (Figures 1 and 2). There was no detectable difference in sedimentation between 70S ribosomes formed from native 30S subunits (Figure 1A) and ribosomes reconstituted from either natural or synthetic 16S rRNA (Figure 1B,C) or from rRNA fragments 1−360/361−1542 and 1−448/449−1542 (Figure 1D,E). Yields of 70S ribosomes from 30S subunits reconstituted with in vitro transcribed 16S rRNA were 4- to 5-fold lower than for natural rRNA but were similar whether the 16S rRNA was provided as a continuous transcript or as two separate fragments (Table 1).

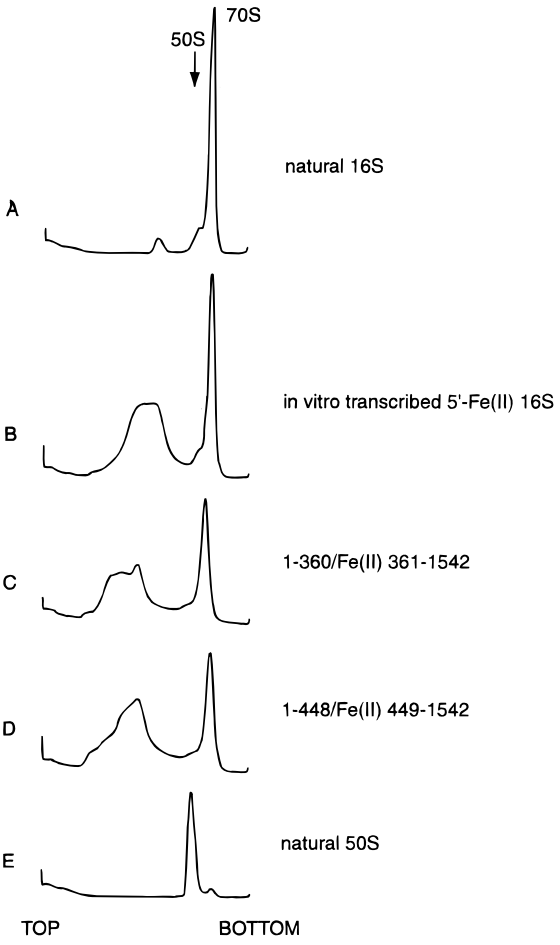

FIGURE 2: Sucrose gradient analysis of 70S ribosomes associated from natural 50S subunits and 30S subunits reconstituted *in vitro* with different constructs of control and modified 16S rRNA: 30S subunits reconstituted with (A) 60 pmol natural 16S rRNA plus 38 pmol 50S subunits, (B) 210 pmol *in vitro* transcribed 5′-Fe(II) 16S rRNA plus 30 pmol 50S subunits, (C) 210 pmol 16S rRNA fragments 1−360 and Fe(II) 361−1542 plus 23 pmol 50S subunits, (D) 210 pmol 16S rRNA fragments 1−448 and Fe(II) 449−1542 plus 23 pmol 50S subunits, and (E) 23 pmol of 50S subunits. Sedimentation is from left to right, and absorbance was monitored at 254 nm.

For each probing experiment, three versions of rRNA were reconstituted. As a first control, 30S subunits were reconstituted from 16S rRNA or fragments of 16S rRNA in which GMP, rather than GMPS, was incorporated at the 5′ end of the 3′ fragment (5′-GMP 16S rRNA, 5′-GMP 361−1542, 5′-GMP 449−1542). These rRNAs were treated with Fe(II)−BABE to control for any cleavage induced independent of GMPS-tethered Fe(II). As a second control, subunits were reconstituted using rRNA containing a nonderivatized GMPS at the 5′ end of the 3′ fragment (5′-GMPS 16S rRNA, 5′-GMPS 361−1542, 5′-GMPS 449−1542). Last, 30S subunits were reconstituted from rRNA in which Fe(II) was tethered to a 5′-GMPS on the 3′ fragment (5′-Fe(II) 16S rRNA, 5′-Fe(II) 361−1542, 5′-Fe(II) 449−1542). The Fe(II)-modified rRNAs are referred to as Fe(II)-1, Fe(II)-361, and Fe(II)-449, respectively. There was no detectable difference in sedimentation behavior when BABE-derivatized rRNA was used for reconstitution.

When *in vitro* transcripts of 16S rRNA are reconstituted using classical reconstitution conditions (*32*), no 30S particles are formed (*20*, *33*). However, 30S particles can be recon-

Table 1: Yield and tRNA Binding Activity of 70S Ribosomes Formed from Reconstituted 30S Subunits in Two Independent Experiments[a]

	unmodified ribosomes			Fe(II)−BABE-modified ribosomes		
30S subunits	% yield of 70S ribosomes[b]	relative tRNA binding with poly(U)[c]	relative poly(U)-independent tRNA binding[c]	% yield of 70S ribosomes[b] or 50S subunits	relative tRNA binding with poly(U)[d]	relative poly(U)-independent tRNA binding[d]
natural 30S	60	1.00	0.33	44	1.00	0.48
reconstituted from natural 16S rRNA	30	0.96	0.39	28	1.10	0.48
in vitro transcribed 16S rRNA	7.8	0.85	0.24	5.4	0.88	0.22
1−360/361−1542	7.6	0.76	0.26	4.3	0.81	0.17
1−448/449−1542	5.7	0.90	0.37	6.0	1.10	0.23
natural 50S subunits	−	0.03[e]	0.02[e]	68[f]	0.13[f]	0.11[f]

[a] Sucrose gradient purification and tRNA binding of ribosomes were performed as described in Materials and Methods. [b] Yield of ribosomes isolated after sucrose gradient sedimentation is based on input rRNA. [c] Values are relative to binding of 1.76 pmol of tRNA bound/pmol of 70S ribosomes formed from natural 30S subunits. [d] Values are relative to binding of 1.20 pmol of tRNA bound/pmol of 70S ribosomes formed from natural 30S subunits. [e] tRNA binding was measured directly on activated 50S subunits, containing less than 2% contamination by 30S subunits. [f] tRNA binding was measured after sucrose gradient sedimentation of 50S subunits isolated along with 70S ribosomes resulting from approximately 5% contamination of the 50S subunits by 30S subunits.

stituted from both natural and *in vitro* transcribed rRNA using a procedure in which the monovalent salt is changed from 330 mM KCl to 500 mM NH_4Cl and an incremental heating procedure is used (*20*, *33*). We further optimized reconstitution of 30S subunits using discontinuous fragments of synthetic rRNA by heating and snap-cooling the rRNA prior to reconstitution (see Materials and Methods). Sucrose gradient analysis of reconstitution experiments in which 16S rRNA and TP30 were titrated showed that a one-to-one molar ratio of rRNA to TP30 gave the greatest amount of 30S subunits (data not shown).

In addition to assaying for the ability of the reconstituted 30S subunits to associate with 50S subunits, we tested the tRNA binding activity of the 70S ribosomes containing both unmodified and Fe(II)−BABE-modified fragmented 16S rRNA. Ribosomes containing unmodified rRNA with an internal break at positions 360/361 of 16S rRNA bound tRNA 0.76 times as efficiently as ribosomes prepared with natural 30S subunits (Table 1). Ribosomes containing underivatized RNA with an internal break at position 448/449 of 16S rRNA bound tRNA 0.90 times as efficiently as ribosomes prepared with natural 30S subunits. Fe(II)−BABE modification did not significantly alter the ability of 70S ribosomes to bind tRNA. Modified ribosomes containing a discontinuity at either position 360/361 or 448/449 bound tRNA 0.81 or 1.1 times, respectively, as efficiently as ribosomes containing natural 30S subunits. At 20 mM $MgCl_2$, poly(U)-independent tRNA binding by all particles was about one-third that observed in the presence of poly(U).

Probing of 70S Ribosomes. Figures 3−5 show autoradiographs of primer extension analyses of 16S rRNA extracted from ribosomes subjected to directed hydroxyl radical probing (*31*). Sites of directed hydroxyl radical cleavage in the RNA backbone appear as bands in lane 3 of the gels. Intensity of cleavage is indicated by the size of the filled circles in Figure 6. The distances between probes and targets can be estimated, based on previously described calibration experiments (*15*). Thus, the distances are predicted to lie within the range of 0−22 Å for strong, 12−36 Å for medium, and 20−44 Å for weak cleavage.

An initial probing experiment was done using 70S ribosomes containing Fe(II) tethered to the 5′ end of full-length 16S rRNA. The rRNA was cleaved near the point of attachment of the probe at nucleotides 2−6 (nucleotide 1 could not be resolved), as shown in Figure 3A and summarized in Figure 6A. Cleavage was also observed in the 620 helix at nucleotides 600−603, 613−616, 632−633, and 636−641 (Figures 3B and 6A).

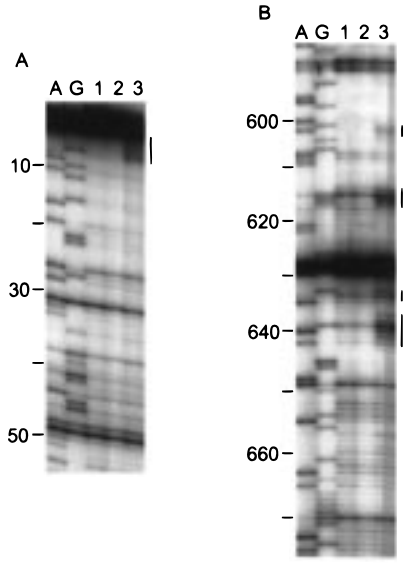

FIGURE 3: Cleavage of 16S rRNA in 70S ribosomes assembled from 30S subunits reconstituted with Fe(II)-1 derivatized 16S rRNA detected by primer extension. A and G are dideoxy sequencing lanes. Lanes 1−3 show directed hydroxyl radical cleavage of 70S ribosomes containing (1) mock-treated GMPS-1 rRNA, (2) Fe(II)−BABE-treated GMP-1 rRNA, and (3) Fe(II)−BABE−GMPS-1 16S rRNA. Hydroxyl radical cleavages are seen as additional bands in lane 3 and are indicated by bars.

Ribosomes containing 16S rRNA fragments 1−360 and 361−1542, with Fe(II) tethered to position 361 of the rRNA, were isolated and probed as described above. Cleavage occurred in the rRNA backbone on both sides of the 27−37/547−556 helix at positions 33−35 and 550−554, as shown in Figure 4A,B and summarized in Figure 6B. Probing from position 361 also resulted in weak cleavage at positions 159−163, 496−497, 512−513, 518−525, 536−538, and stronger cleavage at nucleotides 613−616 (Figures 4B−D and 6B). Finally, the rRNA backbone was cleaved in the middle of the penultimate stem, on both sides of the helix, at positions 1408−1412, 1420−1424, 1478−1481, and 1488−1493 (Figures 4E,F and 6B). The strongest cleavage was observed at nucleotides 1422 and 1423.

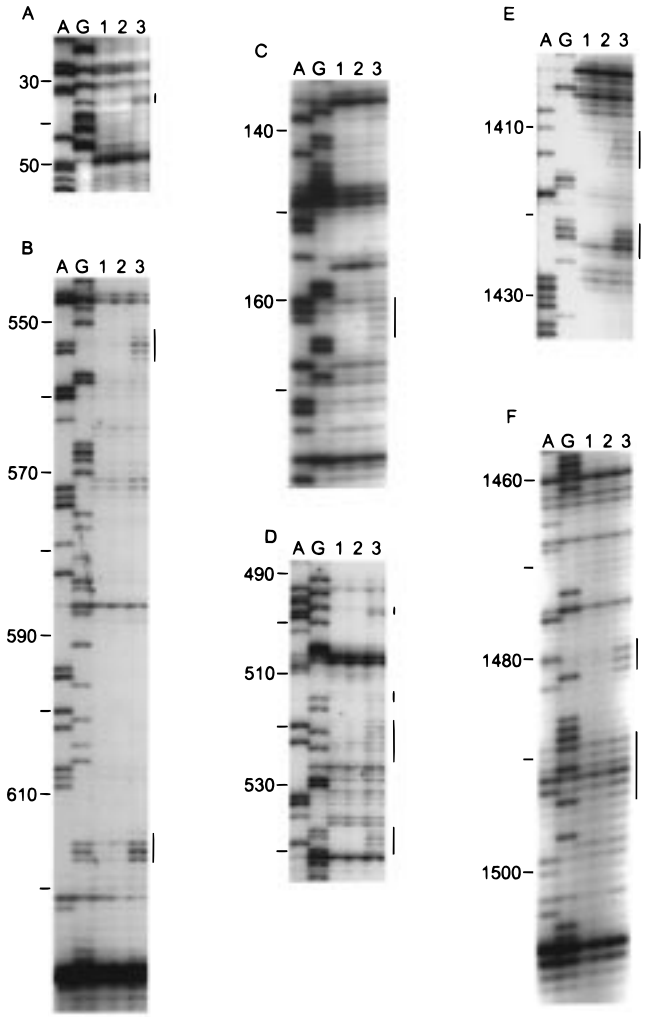

FIGURE 4: Cleavage of 16S rRNA in 70S ribosomes assembled from 30S subunits reconstituted with 16S rRNA fragments 1−360 and Fe(II)-derivatized 361−1542 detected by primer extension. A and G are dideoxy sequencing lanes. Lanes 1−3 show directed hydroxyl radical cleavage of 70S ribosomes containing (1) mock-treated GMPS-361 rRNA, (2) Fe(II)−BABE-treated GMP-361 rRNA, and (3) Fe(II)−BABE−GMPS-361 rRNA. Hydroxyl radical cleavages are seen as additional bands in lane 3 and are indicated by bars.

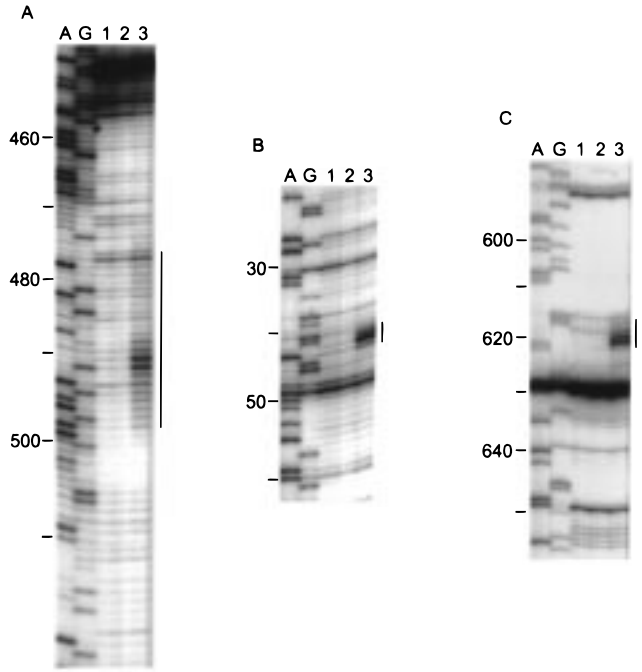

FIGURE 5: Cleavage of 16S rRNA in 70S ribosomes assembled from 30S subunits reconstituted with 16S rRNA fragments 1−448 and Fe(II)-derivatized 449−1542 detected by primer extension. A and G are dideoxy sequencing lanes. Lanes 1−3 show directed hydroxyl radical cleavage of 70S ribosomes containing (1) mock-treated GMPS-449 rRNA, (2) Fe(II)−BABE-treated GMP-449 rRNA, and (3) Fe(II)−BABE−GMPS-449 rRNA. Hydroxyl radical cleavages are seen as additional bands in lane 3 and are indicated by bars.

Hydroxyl radical probing in ribosomes containing 16S rRNA fragments 1−448 and 449−1542, with Fe(II) tethered to position 449, results in cleavage of the 16S rRNA backbone in the opposite strand from the one bearing the Fe(II) probe. Cleavage occurred at positions 474−497, with the strongest cleavage at 489 and 490 (Figures 5A and 6C). Strong cleavage was also detected in a neighboring helix at positions 41−43 (Figures 5B and 6C). Finally, cleavage was observed in the central domain at positions 614−619 (Figures 5C and 6C).

DISCUSSION

Given the high degree of structural complexity of the 30S ribosomal subunit, it is remarkable that two synthetic fragments of 16S rRNA are able to associate with the 21 30S ribosomal proteins (TP30) in vitro to form functional ribosomal subunits. We found two different sets of fragments of 16S rRNA (1−360/361−1542 and 1−448/449−1542) that are able to assemble into active 30S subunits. Although other pairs of fragments of 16S rRNA do not, in our hands, reconstitute into 30S particles, we believe that this approach is sufficiently general to study RNA−RNA proximities at many other sites within 16S rRNA. An advantage of this approach is that probing can be targeted specifically to regions of 16S rRNA for which little structural information is available. Such constraints will be especially helpful in refinement of models for the structure of the 30S subunit.

An alternative method for studying RNA−RNA proximities in 16S rRNA was recently described (*7*). In this cross-linking study, natural 16S rRNA was cleaved specifically using ribonuclease H digestion and a photolabel was introduced at the site of cleavage without separating or denaturing the RNA fragments. After reconstitution of 30S subunits with the modified rRNAs, two cross-links were identified in the 16S rRNA. Data obtained using this cross-linking approach should complement data obtained from directed hydroxyl radical probing. The different techniques utilized to create discontinuities in the rRNA may allow for generation of structural constraints from different sites in the rRNA. For instance, while 30S subunits could not be reconstituted from natural rRNA containing a break between 359 and 360 (*7*), in vitro transcribed rRNA with a discontinuity one nucleotide away could be reconstituted into active 30S subunits in the present studies.

When using particles assembled in vitro for structural probing, it is important to control for the structural integrity of the particles. We have used two functional assays as a stringent test for accurate assembly of 30S subunits. First, only 30S ribosomal subunits capable of associating with natural 50S subunits were selected. Second, the isolated 70S ribosomes containing both full-length or discontinuous in

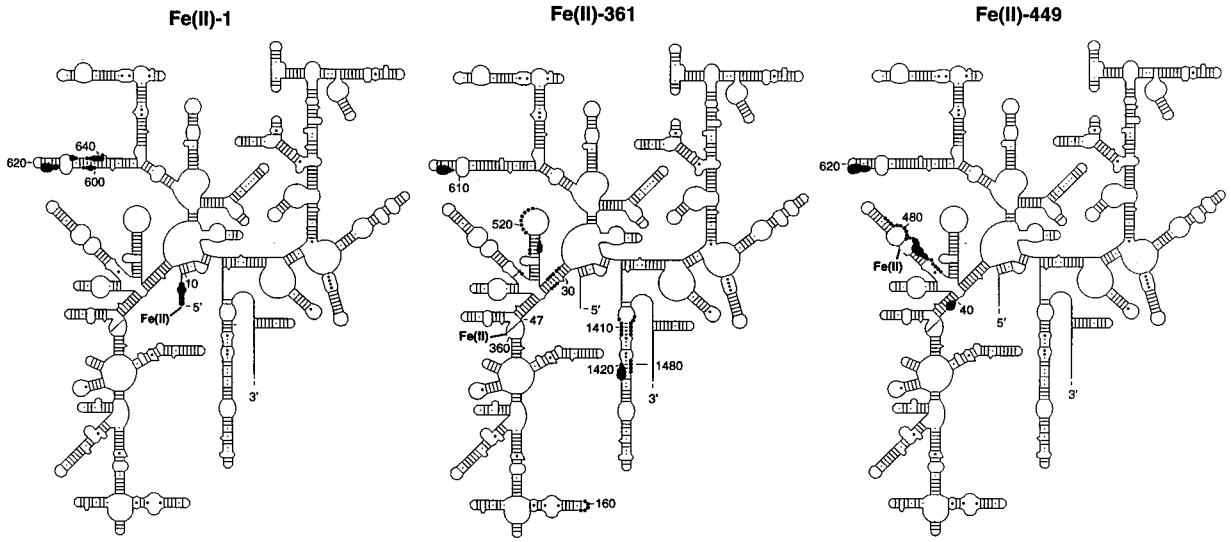

FIGURE 6: Secondary structure of 16S rRNA summarizing the sites of directed hydroxyl radical cleavage from (A) Fe(II)-1 16S rRNA, (B) Fe(II)-36116S rRNA, and (C) Fe(II)-449 16S rRNA. The sizes of the circles correspond to the intensities of cleavage seen at each target site.

vitro transcribed 16S rRNA bound tRNA in an mRNA-dependent manner nearly as efficiently as natural 30S subunits (Table 1). These data, in addition to their sedimentation properties, provide strong evidence that 30S subunits reconstituted from in vitro transcribed 16S rRNA containing discontinuities at positions 360/361 and 448/449 are similar in structure to natural 30S subunits.

A potential concern with this approach is whether the nucleotide to which the probe is tethered has increased mobility due to the discontinuity in the RNA backbone. While it is difficult to address this question unequivocally, our data suggest that the positions of the derivatized nucleotides at positions 1, 361, and 449 resemble those found in natural ribosomes. First, cleavage on the opposite strand of the helix from nucleotide 449, around position 489 (Figure 6C), provides evidence that this helix is constrained to something resembling its correct native structure. Second, if the RNA and tethered probe had a high degree of mobility, we would expect to see only weak cleavage distributed over a wide range of targets. The fact that strong cleavage of 16S rRNA is observed from all three probing positions is indicative that the probe must spend a significant amount of time in one position. The specificity of our cleavage data suggest that movement of the probes and associated rRNA are limited. Finally, as discussed below, the probing results themselves are consistent with earlier studies bearing on the surroundings of the probing positions.

Directed hydroxyl radical probing from Fe(II) tethered to position 1 of 16S rRNA results in cleavage of the RNA backbone at the 5′ end of the RNA (positions 2−6) and at interdigitated sites in the middle of the 620 helix (Figure 6A). There is a significant amount of overlap between this cleavage pattern and that observed with directed hydroxyl radical probing from position 99 of ribosomal protein S5 (*12*; G. Culver, unpublished data). While the 8-nucleotide-long, single-stranded 5′ end of 16S rRNA may be flexible, these two independent experiments place the 5′ end of 16S rRNA in proximity to the middle of the 620 helix in 70S ribosomes. Protein S5 is one of the four 30S ribosomal proteins that has been cross-linked to the 5′ end of 16S rRNA (*6*), and nucleotide 6 is protected from chemical modification by S5 (*34*), providing further evidence for the proximity of the 5′ end of the rRNA to S5.

Nucleotide 361 is located in an internal loop at a three-way helical junction in the 5′ domain of 16S rRNA. The previous structural information for this internal loop and the neighboring, highly conserved 52−58/354−359 helix was insufficient to constrain the three-dimensional positions of these features with confidence. Hydroxyl radicals generated from Fe(II) tethered to nucleotide 361 cleave the RNA backbone of the 27−37/547−556 helix in a 3′-staggered manner (Figure 6B), suggesting that position 361 faces the minor groove of this helix. These data are consistent with previous studies regarding the folding of this region of the 16S rRNA. A phylogenetically predicted tertiary base pair between C47 and G361 (*3*), and a UV cross-link in natural 30S subunits between positions 31 and 48 (*35*), provided earlier evidence for the proximity of positions 31 and 361.

Cleavage of the penultimate stem by hydroxyl radicals generated from Fe(II) tethered to nucleotide 361 constrains one of the most elusive features of 16S rRNA. The most intense cleavages from Fe(II)-361 in this region are observed at positions 1422−3 (Figure 6B), placing nucleotide 361 close to the middle of the penultimate stem. As shown in Figure 6B, the two sets of cleavages in the penultimate stem are spaced 10−12 nucleotides, or one helical turn, apart. The cleavage pattern is again 3′-staggered, suggesting that nucleotide 361 faces the minor groove of these regions of the penultimate stem. It is interesting that the sites of cleavage are interdigitated with nucleotides which, upon subunit association, are protected from cleavage by solution probing with hydroxyl radicals (*36*). These data locate the penultimate stem between the 360 loop and the 50S subunit. Strong cleavage from Fe(II)-361 is also observed around position 615 (Figure 6B). Thus we infer that the 360 loop and its flanking helices lie in the interior of the body of the 30S subunit between the end of the 620 helix and the penultimate stem.

Nucleotide 449 is in an internal loop in the middle of a long, phylogenetically variable helix for which there was little structural information. Previously, it was shown that nucleotides 438−440 in the proximal end of the helix are protected

by ribosomal protein S4 (*37*) and that positions 449 and 453 in the middle of the helix are protected by S16 (*5*) from hydroxyl radicals in solution. In our experiments, probing from position 449 causes strong cleavage of the RNA backbone at nucleotide 42 (Figure 6C), which suggests that nucleotides 449 and 42 are in close proximity. The helix containing position 42 extends from the helical junction where S4 binds, in the body of the subunit (*11*, *37*, *38*). The end of the 620 helix, which is also cleaved from Fe(II)-449 (Figure 6C), is also positioned in the body of the subunit (*4*; H.F.N., unpublished data). Therefore, our data constrain the loop containing nucleotide 449 to the body of the subunit near both position 42 and the end of the 620 helix.

Interestingly, the 5′ strand of the 620 helix, around position 615, is cleaved from all three probing positions described here. This finding is consistent with previous footprinting studies, which show that protein S16 protects the end of the 620 helix, as well as nucleotides near all three probing positions, from attack by chemical probes (*5*, *39*). Moreover, the targets of cleavage by directed probing from the 5′ end of 16S rRNA, position 361, and position 449 in several cases flank the sites of protection by S16 (*5*), including nucleotides around positions 610 and 630, around positions 32, 48, and 450, and, more weakly, around positions 10 and 40. Thus, several independent studies place all of these regions of rRNA near the end of the 620 helix. Since there are virtually no other overlapping targets from the three probing sites, we infer that the end of the 620 helix is approximately equidistant from the 5′ end of 16S rRNA, nucleotide 361, and nucleotide 449.

These studies demonstrate that directed hydroxyl radical probing from Fe(II) tethered to 16S rRNA can be used to determine RNA−RNA proximities. The constraints generated are currently being used to refine our model of the folding of 16S rRNA in the 30S subunit. Additional studies using directed probing from other poorly constrained regions of the rRNA should allow prediction of the folding, at low resolution, of the entire 16S rRNA structure.

ACKNOWLEDGMENT

We thank Gloria Culver, Lovisa Holmberg, Kate Lieberman, and Kevin Wilson for critical comments on the manuscript; members of the Noller lab for helpful discussions; S. Joseph for advice on tethering to 5′-GMPS RNA; and J. Moran, D. P. Greiner, and S. Joseph for 1-(*p*-bromoacetamidobenzyl)-EDTA, which was synthesized in the laboratory of C. Meares.

REFERENCES

1. Noller, H. F., and Woese, C. R. (1981) *Science 212*, 403−411.
2. Woese, C. R., Gutell, R., Gupta, R., and Noller, H. F. (1983) *Microbiol. Rev. 47*, 621−669.
3. Gutell, R. R., Larsen, N., and Woese, C. R. (1994) *Microbiol. Rev. 58*, 10−26.
4. Stern, S., Weiser, B., and Noller, H. F. (1988) *J. Mol. Biol. 204*, 447−481.
5. Powers, T., and Noller, H. F. (1995) *RNA 1*, 194−209.
6. Brimacombe, R. (1991) *Biochimie 73*, 927−936.
7. Baranov, P. V., Dokudovskaya, S. S., Oretskaya, T. S., Dontsova, O. A., Bogdanov, A. A., and Brimacombe, R. (1997) *Nucl. Acids Res. 25*, 2266− 2273.
8. Mueller, F., and Brimacombe, R. (1997) *J. Mol. Biol. 271*, 524−544.
9. Wilms, C., Noah, J. W., Zhong, D., and Wollenzien, P. (1997) *RNA 3*, 602−612.
10. Capel, M. A., Engelman, D. M., Freeborn, B. R., Kjeldgaard, M., Langer, J. A., Ramakrishnan, V., Schindler, D. G., Schneider, D. K., Schoenborn, B. P., Sillers, I.-Y., Yabuki, S., and Moore, P. B. (1987) *Science 238*, 1403−1406.
11. Heilek, G. M., Marusak, R., Meares, C. F., and Noller, H. F. (1995) *Proc. Natl. Acad. Sci. USA 92*, 1113−1116.
12. Heilek, G. M., and Noller, H. F. (1996) *Science 272*, 1659−1662.
13. Heilek, G. M., and Noller, H. F. (1996) *RNA 2*, 597−602.
14. Joseph, S., and Noller, H. F. (1996) *EMBO J. 15*, 910−916.
15. Joseph, S., Weiser, B., and Noller, H. F. (1997) *Science 278*, 1093−1098.
16. Wilson, K. S., and Noller, H. F. (1998) *Cell 92*, 131−139.
17. Hubbard, J. M., and Hearst, J. E. (1991) *J. Mol. Biol. 221*, 889−907.
18. Malhotra, A., and Harvey, S. C. (1994) *J. Mol. Biol. 240*, 308−340.
19. Fink, D. L., Chen, R. O., Noller, H. F., and Altman, R. B. (1996) *RNA 2*, 851−866.
20. Krzyzosiak, W., Denman, R., Nurse, K., Hellmann, W., Boublik, M., Gehrke, C. W., Argis, P. F., and Ofengand, J. (1987) *Biochemistry 26*, 2353−2364.
21. Weitzmann, C. J., Cunningham, P. R., Nurse, K., and Ofengand, J. (1993) *FASEB 7*, 177−180.
22. Agalarov, S. C., Zheleznyakova, E. N., Selivanova, O. M., Zheleznaya, L. A., Matvienko, N. I., Vasiliev, V. D., and Spirin, A. S. (1998) *Proc. Natl. Acad. Sci. USA 95*, 999−1003.
23. Samaha, R. R., O'Brien, B., O'Brien, T. W., and Noller, H. F. (1994) *Proc. Natl. Acad. Sci. U.S.A. 91*, 7884−7888.
24. DeRiemer, L. H., Meares, C. F., Goodwin, D. A., and Diamanti, C. J. (1981) *J. Labeled Compd. Radiopharm. 18*, 1517−1534.
25. Moazed, D., Stern, S., and Noller, H. F. (1986) *J. Mol. Biol. 187*, 399−416.
26. Nierhaus, K. H. (1990) in *Ribosomes and Protein Synthesis* (Spedding, G., Ed) pp 161−189, Oxford University Press, Oxford, U.K.
27. Triman, K., Becker, E., Dammel, C., Katz, J., Mori, H., Douthwaite, S., Yapijakis, C., Yoast, S., and Noller, H. F. (1989) *J. Mol. Biol. 209*, 645−653.
28. Milligan, J. F., Duncan, R. G., Witherell, G. W., and Uhlenbeck, O. C. (1987) *Nucl. Acids Res. 15*, 8783−8798.
29. Sampson, J. R., and Uhlenbeck, O. C. (1988) *Proc. Natl. Acad. Sci. U.S.A. 85*, 1033−1037.
30. Sampson, J. R., DiRenzo, A. B., Behlen, L. S., and Uhlenbeck, O. C. (1989) *Science 243*, 1363−1366.
31. Stern, S., Moazed, D., and Noller, H. F. (1988) *Methods Enzymol. 164*, 481−489.
32. Held, W. A., and Nomura, M. (1973) *Biochemistry 12*, 3273−3281.
33. Denman, R., Weitzmann, C., Cunningham, P. R., D., N., Nurse, K., Colgan, J., Pan, Y.-C., Miedel, M., and Ofengand, J. (1989) *Biochemistry 28*, 1002−1011.
34. Stern, S., Powers, T., Changchien, L.-M., and Noller, H. F. (1988) *J. Mol. Biol. 201*, 683−695.
35. Stiege, W., Atmadja, J., Zobawa, M., and Brimacombe, R. (1986) *J. Mol. Biol. 191*, 135−138.
36. Merryman, C., McWhirter, J., and Noller, H. F. *J. Mol. Biol.*, in press.
37. Powers, T., and Noller, H. F. (1995) *J. Biol. Chem. 270*, 1238−1242.
38. Stern, S., Wilson, R. C., and Noller, H. F. (1986) *J. Mol. Biol. 192*, 101−110.
39. Stern, S., Changchien, L.-M., Craven, G. R., and Noller, H. F. (1988) *J. Mol. Biol. 200*, 291−299.

BI981644A